

## GAIN SCHEDULING CONTROL FOR THE HYDRAULIC ACTUATION OF THE HYQ ROBOT LEG

Thiago B. Cunha<sup>1,2</sup>, boaventura@emc.ufsc.br  
Claudio Semini<sup>1</sup>, claudio.semini@iit.it  
Emanuele Guglielmino<sup>1</sup>, emanuele.guglielmino@iit.it  
Victor J. De Negri<sup>2</sup>, victor@emc.ufsc.br  
Yousheng Yang<sup>1</sup>, yousheng.yang@iit.it  
Darwin G. Caldwell<sup>1</sup>, darwin.caldwell@iit.it

<sup>1</sup> Italian Institute of Technology – Advanced Robotics Department – Via Morego 30, Genoa, Italy

<sup>2</sup> Federal University of Santa Catarina – LASHIP – Campus Universitário, Trindade, Florianópolis – SC, Brazil

**Abstract.** *This paper focuses on a theoretical and experimental investigation on the control of a valve actuated hydraulic system driving a biologically inspired robotic leg. The study is part of a more complex project aiming at the design of a power and cognitive autonomous quadruped robot for outdoor operations called HyQ. The first leg prototype has currently two hydraulically activated degrees of freedom (DOF) actuating the hip and knee joints. Hydraulic actuation has been chosen in lieu of electrical, due to its high power-to-weight ratio and fast dynamic response, to meet the specifications in terms of performance and dimensions. The actuation system is composed of a proportional valve and an asymmetric cylinder (one for each DOF). Non-linear and linear system modelling and identification have been undertaken. The measured response in the time domain has been compared with the results of numerical simulation both in the linear and non-linear cases. An initial control implementation has been carried out. A gain scheduling algorithm has been implemented where PID controller gains are adapted according to the joint position within a walking trajectory cycle. The performance of this adaptive controller has been compared with a conventional PID control scheme.*

**Keywords:** *legged robotics, hydraulic actuation, bio-inspired design, adaptive control, gain scheduling*

### 1. INTRODUCTION

Bio-inspired autonomous robotics is at the forefront of today's robotics research and particularly legged robots (*e.g.*, humanoids, quadrupeds) are being extensively investigated. The results reported in this paper are within the framework of a more complex multi-disciplinary project aiming at developing a hydraulically-actuated power and cognitive autonomous quadruped robot, named HyQ (Semini et al., 2008) with overall dimensions comparable to a large dog or a small horse.

The main purpose of the HyQ project is to develop a robot able to walk, run and jump, and move autonomously outdoors. It can find application in tasks such as carrying heavy loads or performing rescue operations in places not reachable with wheeled vehicles or helicopters. Furthermore, it will constitute a platform to study and test the applicability of fluid power to actuate legged robots and to investigate high efficiency hydraulic drives. It will also serve as experimental platform to conduct research on biologically-inspired locomotion, in particular gait pattern generation and stability.

Robotics is typically associated with electrical actuation (*e.g.*, brushed and brushless DC motors). However, the need to cope with heavy loads and respond quickly to external inputs and disturbances has recently caused a renewed interest in hydraulic power and its use in robotics. Hydraulic actuation systems have high power-to-weight ratio, swift dynamic response and are able to work reliably in outdoor environments. This renewed interest has occurred despite the fact that for several years, within the robotics community, hydraulic drives have been generally considered not to be fit for the dynamic control challenges in robotic locomotion due to the difficulty in their control.

It should be noticed that the early days of legged robots were dominated by hydraulic systems such as the GE quadruped robot by Liston and Mosher (1968). Pioneering research in the area of fluid power (both pneumatic and hydraulic) actuation for legged locomotion was carried out by Raibert (1984a and 1984b), who produced several running robots, including mono, bi and quadruped systems. The biologically-inspired hopping robot Kenken (Hyon et al., 2003) had an articulated leg composed of three links. It used two hydraulic actuators as muscles and linear springs as tendons. Work by Hyon and Cheng (2007) at ATR Computational Neuroscience Laboratories in Japan and Bentivegna and Atkeson (2007) at Carnegie Mellon University in the USA have recently shown this technology applied to advanced humanoid robots. Recently the work on BigDog, by Boston Dynamics (Raibert et al., 2008) has shown remarkable potential for fluid power as a mean to actuate robots.

The proportional-integral-derivative (PID) controller is by far the most commonly used controller. About 90% to 95% of all control problems are solved by this controller. This predominance is basically due to its simplicity and good behaviour in closed loop. Usually, in hydraulic subsystems the PID controller also achieves a satisfactory performance. However, if the process dynamics are changing (*e.g.*, by nonlinearities in the control loop), it is useful to compensate

for these changes by changing the controller. If the variations can be predicted from measured signals, gain scheduling should be used since it is simpler and gives superior and more robust performance than continuous adaptation (Levine, 1995).

In this paper the modelling and two control schemes for a hydraulically-actuated robotic leg are presented. The paper is organised as follows: section 2 introduces the design of the quadruped robot leg and its actuation system. Section 3 focuses on the system modelling (hydraulic system and leg) and section 4 on the controller design. Section 5 is concerned with the simulation and a preliminary experimental study. Finally, section 6 addresses the conclusions and comments on further developments.

## 2. SYSTEM DESIGN

### 2.1. Bio-inspired leg design

The robotic leg should enable natural, stable, robust actions as found in quadruped animals. From a biological perspective advanced locomotion abilities (*e.g.*, running and jumping) have been thoroughly studied in cats (and felids in general), dogs and horses. These studies were the starting point for the bio-inspired design of the leg.

Each leg has three actuated DOF: two in the hip (sagittal and frontal plane) and one in the knee (sagittal plane). Figure 1 depicts the first prototype, built in aluminium alloy and stainless steel. The leg mass and inertia were reduced as much as possible, as this positively impacts on the power requirements.

The range of motion of the two DOF in the sagittal plane is biologically inspired (Semini et al., 2008). Both hip/shoulder and knee/elbow flexion/extension joints of the HyQ leg prototype are able to rotate  $120^\circ$ . The range of motion of the third DOF, which is the motion of the hip joint (ab/adduction) in the frontal plane, is set to  $90^\circ$ . This allows the robot to stabilise its body and retain its balance in case of disturbances from the side. The first version of the HyQ leg prototype consists of two limb segments: the femur and the tibia. Each of them has a length of  $0.3\text{ m}$ . For initial tests the frontal plane DOF is inactive and the leg has been constrained to a vertical slider as shown in Fig. 1.



Figure 1. Picture of the HyQ leg prototype (version 1) and its hydraulic actuation fixed to a vertical slider

As occurs in nature, in order to increase the gait efficiency through potential energy storage and release in elastic elements, some passive leg compliance was introduced. This was achieved in this first version by designing a foot in viscoelastic rubber linked with a spring.

### 2.2. Leg actuation design

HyQ uses double-acting linear hydraulic actuators because of their compactness, low weight, and high force capabilities. The fast response specification is met due the low compressibility of hydraulic fluids, which gives a relative high control bandwidth (Semini et al., 2008).

The locomotion trajectories (gait patterns) for the different locomotion modes can be simplified as periodical waveforms whose fundamental frequencies are in the order of  $1\text{ Hz}$  (in walking mode) up to  $2\text{-}3\text{ Hz}$  (in running mode) hence proportional valves with overlap were chosen (bandwidth around  $30\text{-}40\text{ Hz}$ ).

The electrohydraulic actuation of the leg consists of two 4-way proportional valves (Wandfluh WDP-F-A03-ACB-S5-G24) supplied by a positive displacement gear pump in parallel with a relief valve. This provides flow to two unequal area hydraulic cylinders (Hoerbiger LB6-1610-0070-4M) controlling the motion of the leg (hip and knee rotations). The variable load from the leg acts on the piston rods. The cylinders are arranged in triangular configurations between the hip and the two leg segments, as can be seen in Fig. 1.

### 3. MODELLING

#### 3.1. Electrohydraulic actuation

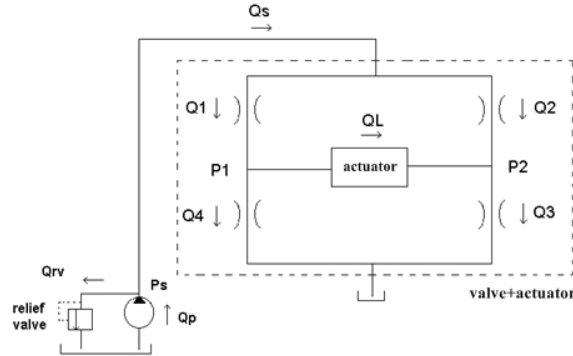


Figure 2. Equivalent hydraulic circuit for each valve-actuator unit

With reference to Fig. 2, showing the electrically equivalent circuit (Wheatstone bridge) for a 4-way valve (Merritt, 1967), flow continuity equation yields for  $P_S > P_{Cr}$  (where  $P_S$  is the supply pressure and  $P_{Cr}$  is the relief valve cracking pressure):

$$Q_p = Q_s + Q_{rv} + Q_c \quad (1)$$

where  $Q_p$  is the rated flow of the pump,  $Q_{rv}$  the flow in the relief valve,  $Q_c$  is the compressibility flow in the line connecting the outlet of the pump with the inlet of the relief valve and with the supply port of each control valve and  $Q_s$  is the flow supplied to the valves and is defined as:

$$Q_s = Q_1 + Q_2 = Q_3 + Q_4 \quad (2)$$

The compressibility flow in the connecting hose is:

$$Q_c = \frac{V_{hose}}{\beta_{eff}} \frac{dP_s}{dt} \quad (3)$$

where  $V_{hose}$  is the volume of the connecting hose and  $\beta_{eff}$  the effective bulk modulus. The effective bulk modulus is a physical property of fluid, which dominates the dynamic phenomena and depends not only on the oil compressibility but also on the free air presence in the oil as well as on the hose elasticity (Merritt, 1967).

The governing equation of the relief valve is:

$$P_s = P_{Cr} + k_{rv}(Q_p - Q_s - Q_c) \quad (4)$$

where  $k_{rv}$  is the relief valve override coefficient.

Oil temperature was assumed to be constant in the model as an air cooler is present in the oil delivery line keeping oil temperature at around 45 °C. The model of the oil used is as close as possible to the oil employed (ISO VG 46).

The flow through orifices is generically obtained applying Bernoulli's equation. If the height variation is negligible and if the fluid velocity downstream the orifice can be neglected with respect to the velocity in the orifice, it can be defined as:

$$Q = c_d A_o \sqrt{\frac{2\Delta P}{\rho}} \quad (5)$$

where  $c_d$  is the discharge coefficient,  $A_o$  is the orifice area,  $\Delta P$  is the pressure difference across the orifice and  $\rho$  the oil density.

In a proportional valve the area  $A_o$  is not a constant but a function of the spool position. Due to the difficulty in obtaining geometrical parameters from the valve datasheet, the partial flow rate coefficient  $k_{vp}$  can be defined as (De Negri et al., 2008):

$$k_{vp} = \frac{c_d A_0(z_n)}{\sqrt{\rho}} = \frac{Q_n}{\sqrt{2\Delta P_n}} \quad (6)$$

where  $Q_n$  is the nominal flow and  $\Delta P_n$  the pressure drop at the nominal flow (which are easily obtained from datasheet information), and  $A_0(z_n)$  is the orifice area on the nominal spool displacement. The nominal displacement is the maximum value in the operation range before the volumetric flow saturation is reached.

The next step in the modelling requires the application of the continuity equation at the valve+actuator subsystem defined in Fig. 2 which yields:

$$Q_L = Q_1 - Q_4 = Q_3 - Q_2 \quad (7)$$

Combining Eq. (5) and Eq. (6), flows through each valve orifice can be expressed as:

$$Q_i = k_{vp} \frac{z}{z_n} \sqrt{2(P_S - P_i)} \quad (8)$$

$$Q_j = k_{vp} \frac{z}{z_n} \sqrt{2(P_{j-2} - P_T)} \quad (9)$$

where  $i = 1$  or  $2$  and  $j = 3$  or  $4$ .  $P_1$ ,  $P_2$  and  $P_T$  are the valve load ports pressure (coinciding with the hydraulic piston chamber pressures if the small pressure losses in the connecting hoses are neglected) and reservoir pressure respectively and  $z$  is the spool position. The spool-solenoid electromechanical dynamics can be expressed through a second-order linear model.

Applying the continuity equation to each actuator yields:

$$Q_1 - L(P_1 - P_2) - A_1 \frac{dx}{dt} = \frac{V_1}{\beta_{eff}} \frac{dP_1}{dt} \quad (10)$$

$$-Q_3 + L(P_1 - P_2) - A_2 \frac{dx}{dt} = \frac{V_2}{\beta_{eff}} \frac{dP_2}{dt} \quad (11)$$

where  $A_1$ ,  $A_2$ ,  $V_1$  and  $V_2$  are respectively the piston end and rod end areas and volumes,  $L$  the piston leakage coefficient and  $x$  the actuator displacement.

Defining the hydraulic force as:

$$F_h = P_1 A_1 - P_2 A_2 \quad (12)$$

and considering Eq. (10) and Eq. (11), the actuator pressure dynamics is given by:

$$\frac{dF_h}{dt} = \frac{A_1 \beta_{eff}}{V_1} \left( Q_1 - L(P_1 - P_2) - A_1 \frac{dx}{dt} \right) - \frac{A_2 \beta_{eff}}{V_2} \left( Q_2 + L(P_1 - P_2) + A_2 \frac{dx}{dt} \right) \quad (13)$$

Finally, the force balance in each cylinder is given by:

$$F_h - F_{friction} - F_L = M \frac{d^2 x}{dt^2} \quad (14)$$

where  $M$  is the load mass,  $F_L$  the variable load force acting on the piston rod (depending on the leg angles position) and  $F_{friction}$  the friction force in the cylinder due to the seals, which is composed of a viscous, a Coulomb, and a stiction term.

The hydraulic parameters are listed in Tab. 1.

Table 1. Key parameters of the hydraulic system.

PARAMETER	VALUE
Pump flow rate	$1.0 \times 10^{-4} \text{ m}^3/\text{s}$
Relief valve cracking pressure	$1.6 \times 10^7 \text{ Pa}$
Piston diameter	$1.6 \times 10^{-2} \text{ m}$
Rod diameter	$1.0 \times 10^{-2} \text{ m}$
Piston area	$2.01 \times 10^{-4} \text{ m}^2$
Piston ring area	$1.23 \times 10^{-4} \text{ m}^2$
Cylinder stroke	$7.0 \times 10^{-2} \text{ m}$
Valve spool resonant frequency	$35 \text{ Hz}$
Valve flow rate at nominal pressure drop over 2 metering edges	$8.33 \times 10^{-5} \text{ m}^3/\text{s} @ 1.0 \times 10^6 \text{ Pa}$
Valve-actuator connecting hose, internal diameter	3/16" (length 0.8 m)
Hydraulic oil type	ISO VG 46
Hydraulic oil density	$860 \text{ kg/m}^3$
Oil temperature	$318 \text{ K}$ (cooler present)
Absolute oil viscosity	$4.6 \times 10^{-4} \text{ Pa}\cdot\text{s}$
Viscous friction coefficient	$500 \text{ N}\cdot\text{s/m}$
Bulk modulus	$3.0 \times 10^8 \text{ Pa}$

### 3.2. Leg dynamics

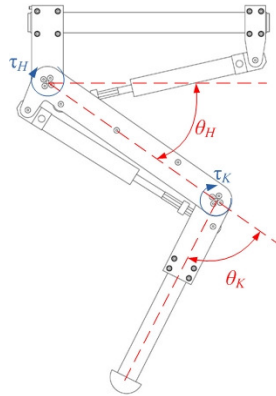


Figure 3. Angle definitions and torque directions for hip and knee

To describe the leg dynamics, a non-linear model was developed using the Euler-Lagrange approach, which gives a relation between torque and angular dynamics (displacement, velocity and acceleration). The system is multiple-input multiple-output (MIMO) and its equations are in general term expressed as:

$$\{\tau(t)\}_{2 \times 1} = [B(q(t))]_{2 \times 2} \{\ddot{q}(t)\}_{2 \times 1} + [C(q(t), \dot{q}(t)) ]_{2 \times 2} \{\dot{q}(t)\}_{2 \times 1} + [G(q(t)) ]_{2 \times 1} \quad (15)$$

where  $q(t)$  is the angular position vector and  $\tau(t)$  is the joint torque vector. The dimensions of matrices and vectors are indicated at their sides.

The contact dynamics with non-holonomic constraint of the ground will not be considered in this work.

### 4. CONTROLLER DESIGN AND IMPLEMENTATION

For quadruped legged locomotion, control performance specifications are determined based on desired locomotion gaits (walk, trot or gallop/bound). Biological studies on quadrupeds revealed that animals choose the gait and preferred forward velocity in order to minimise energy consumption (Hoyt and Taylor, 1981).

In terms of control in the robotic and fluid power literature a vast number of algorithms have been proposed to tackle the non-linear behaviour of multi-body robotic links and hydraulic servo-systems. Robotic researchers investigated a variety of controlled actuators to design joints with both strong and compliant properties (Hayward, 1994; Namvar and Aghili, 2003; Luca, et al., 2006; Palli, et al., 2007). Hyon and Cheng (2006a and 2006b) employed joint torque control in all joints of a hydraulically actuated humanoid robot. They achieved stable control, gravity compensation, and good robot balancing properties.

By surveying the fluid power engineering literature and practice it can be noticed that in hydraulics a reasonably good accuracy can generally be obtained with a PID controller if the load is stationary or moving at low speed (Jacazio and Bassolini, 2005). Adaptive control can potentially be used (Krus and Gunnarson, 1993), however, fast adaptation is required as well as good quality sensors; nevertheless sometimes fluid borne noise hampers controller expected performance. Work has been done on gain scheduling schemes, where the gains of the controller are changed while the device is operating to meet the demanded dynamic performance (Jarrah and Al-Jarrah, 1999; Paijmans et al., 1999). Robust controllers (*e.g.*,  $H_\infty$  control) offer potential solutions but yield complicated to design controllers, while sliding mode control (and other switching-type controllers) may excite higher order vibrating modes because of their inherent chattering (Kachroo and Tomizuka, 1996). Linjama and Virvalo (2005), investigated lower-order robust controllers, which offer a reasonable trade-off between performance and complexity. They found that a filtered proportional controller (proportional plus first order lag) can provide satisfactory performance and a reasonable amount of robustness also with a variable loading.

#### 4.1. PID tuning

In order to design a baseline PID controller a linearisation of the leg dynamics and hydraulic actuation system was carried out. Initially, a single-input single-output (SISO) model for the leg was obtained neglecting the mutual influence of each joint. Friction forces were neglected too. A seventh-order system (angle displacement-to-valve input voltage transfer function) was obtained and the PID tuned.

It was decided to implement a position control loop feeding back joint angular displacements using high resolution encoders. The controller design requirements for the hip and knee were chosen based on the step response as follows: rise time (80%) of 0.3 s, settling time (5%) of 0.5 s and maximum overshoot of 10%. However, the derivative gain obtained with this simplified model was much higher than expected. This was due to the lack of natural damping in the model because of the above approximation. This very high derivative gain was acting as an artificial damping in the system.

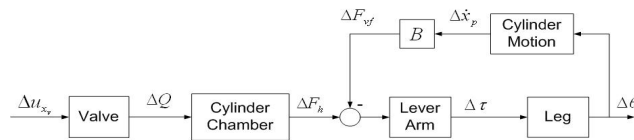


Figure 4. Open-loop linear model block diagram for each cylinder

The linear model was improved considering also the viscous friction in the hydraulic cylinders. This resulted in an internal feedback loop in the above model (see Fig. 4, where  $B$  is the viscous friction coefficient) and a ninth-order system was obtained. The PID was re-calculated and the obtained derivative gain was more consistent with the expected one. These gains are listed in the second row of Tab. 2 (named PID 2).

#### 4.2. Gain scheduling

Since the linearisation is made around an equilibrium point, the PID works properly near this point while far from it the tracking error increases. In order to improve the performance of the control, a gain scheduling scheme was designed.

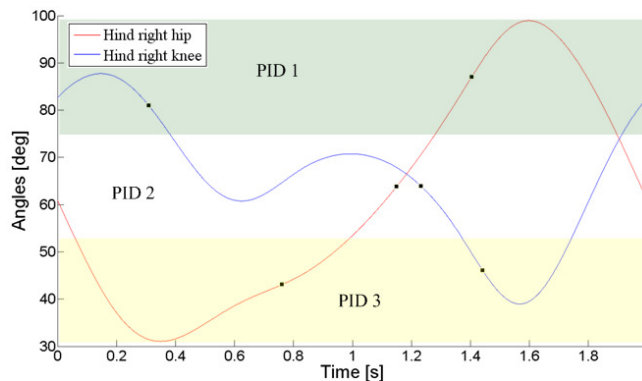


Figure 5. Hip and knee angles in an animal-walking cycle and PID workspaces

Based on the so-called composite cycloid foot trajectory (Sakakibara et al., 1990) the periodical hip and knee joint trajectories of a slowly walking animal leg have been generated (Fig. 5). These trajectories have been analysed to obtain

three PID workspaces (green, white, and yellow areas in Fig. 5). The workspace borders were chosen in order to avoid consecutive undesired switches in the controller gains within a short time period (chattering). Furthermore, the angular positions to make the linearisation (black squared dots in Fig. 5) were taken as the average point within the angular variation in the workspace (e.g., in the PID 1 workspace, the knee angle changes from  $88^\circ$  to  $74^\circ$  and the average point is  $81^\circ$ ). Then a linearisation was carried out resulting in three different linear models. A PID controller was tuned for each of them adding basic adaptive features to the control system. The obtained gains are listed in Tab. 2.

Table 2. PID gain scheduling.

	Hip			Knee		
	$k_p$	$k_i$	$k_d$	$k_p$	$k_i$	$k_d$
PID 1 ( $\theta_H = 87^\circ$ and $\theta_K = 81^\circ$ )	3.4	2	0.0034	4	2	0.002
PID 2 ( $\theta_H = 64^\circ$ and $\theta_K = 64^\circ$ )	4	2	0.004	3.4	2	0.002
PID 3 ( $\theta_H = 43^\circ$ and $\theta_K = 46^\circ$ )	5	2	0.006	3	2	0.002

### 4.3. Digital controller implementation

Proportional flow metering in the spool valves is achieved driving them with a PWM signal at a frequency of  $2\text{ kHz}$ . The PWM signal is generated by the control software that is executed on a PC-104 based platform connected to a Sensoray 526 data acquisition board (DAQ). The DAQ board is also equipped with eight 16-bit A/D converter used for the data acquisition of the sensors. The control loop frequency (i.e., the sampling frequency) has been set to  $1\text{ kHz}$ .

Since the leg control is implemented in software, a digital PID is necessary. An ideal PID in a parallel form (Levine, 1995) can be converted into the discrete domain (sampling time  $T_s$ ) considering a rectangular approximation for the integral and a first-order difference for the derivate. Thus, the digital version of the PID is described by:

$$u(kT_s) = P(kT_s) + I(kT_s) + D(kT_s) \quad (16)$$

where  $k$  is a natural number and  $u(kT_s)$  the control action at the instant  $kT_s$ . It is composed of  $P(kT_s)$ ,  $I(kT_s)$ ,  $D(kT_s)$  which are respectively the proportional, integral and derivative control actions at the instant  $kT_s$  and are given by:

$$P(kT_s) = k_p e(kT_s) \quad (17)$$

$$I(kT_s) = I((k-1)T_s) + k_i T_s \left( \frac{e(kT_s) + e((k-1)T_s)}{2} \right) \quad (18)$$

$$D(kT_s) = \frac{k_d}{T_s} (e(kT_s) - e((k-1)T_s)) \quad (19)$$

where  $e(kT_s)$  is the tracking error at the instant  $kT_s$ .

## 5. EXPERIMENTAL WORK AND MODEL VALIDATION

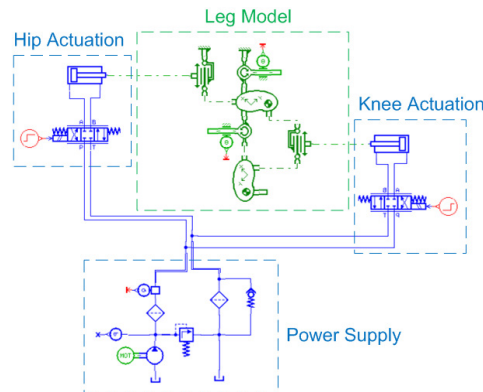


Figure 6. System (leg+hydraulics) model implemented in the LMS Imagine.Lab AMESim software package

For experimental studies the leg was fixed to a table, so that the foot did not touch the ground. Both actuators were supplied with hydraulic fluid, with the control valves mounted on a single manifold, depicted in Fig. 1.

As the major limiting factor in the system is the response of the actuation and in particular of the valve, before assessing the performance of the whole system, a bench test assessment was undertaken on the valve separately in order to measure its performance since the datasheet did not provide all the characteristics required to fully identify the behaviour of the valve under dynamic conditions.

The pressure gain (*i.e.*, the curve slope on the pressure-to-input voltage graph) was first measured (graph not reported here) blocking the two load ports of the valve and applying a low frequency sinusoidal signal. This was useful to assess the effective amount of overlap, in order to compensate it in the control software with an appropriate inverse non-linearity. Dynamic performance was assessed via frequency response analysis. Figure 7 shows the Bode diagram of the output pressure-to-solenoid input voltage transfer function which has a cut-off frequency of about 35 Hz. This parameter was used to obtain the linear valve model (see Fig. 4). A third-order lag approximates the measured response sufficiently well (dashed line in Fig. 7).

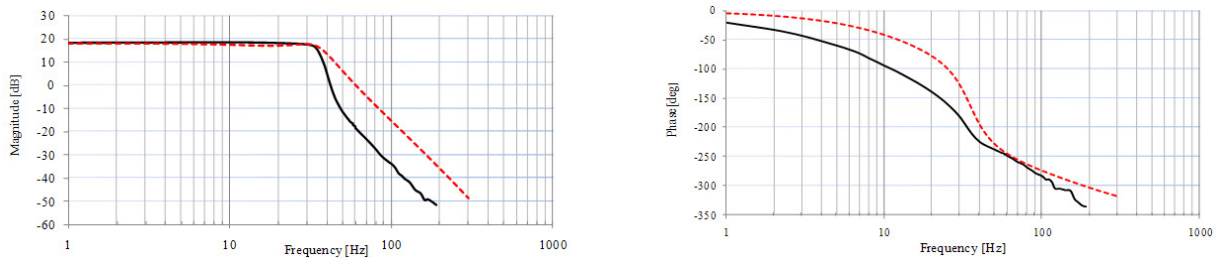


Figure 7. Valve pressure-to-voltage Bode diagram: experiments (solid) and simulation (dashed)

The dynamic experimentation on the valve aimed at identifying how its bandwidth depended upon varying the stimulus amplitude, and supply pressure. Results (not displayed here) showed that the variation on the voltage input and supply pressure did not affect majorly the response. Effective bulk modulus was estimated to be  $3.0 \times 10^8 \text{ Pa}$  (as opposed to the theoretical value of  $1.6 \times 10^9 \text{ Pa}$  for a hydraulic fluid).

Having identified the hydraulic drive performance and having assessed that the bandwidth and the amount of non-linearity were both acceptable, a gain scheduling based on a piecewise linear PID controller was designed.

When the controller was implemented, at first in the non-linear model, and subsequently in the real system, the gains obtained in section 4.1 were readjusted to reduce the trajectory tracking error and in this first implementation to reduce the risk of damaging the leg. The scale factor used to implement the gains obtained with the linear model in the software and in the non-linear model was 0.30 for the hip and 0.80 for the knee. As a PID controller has zero steady state error only for a step reference, any other reference trajectory results in a tracking error between the output and the reference trajectory.

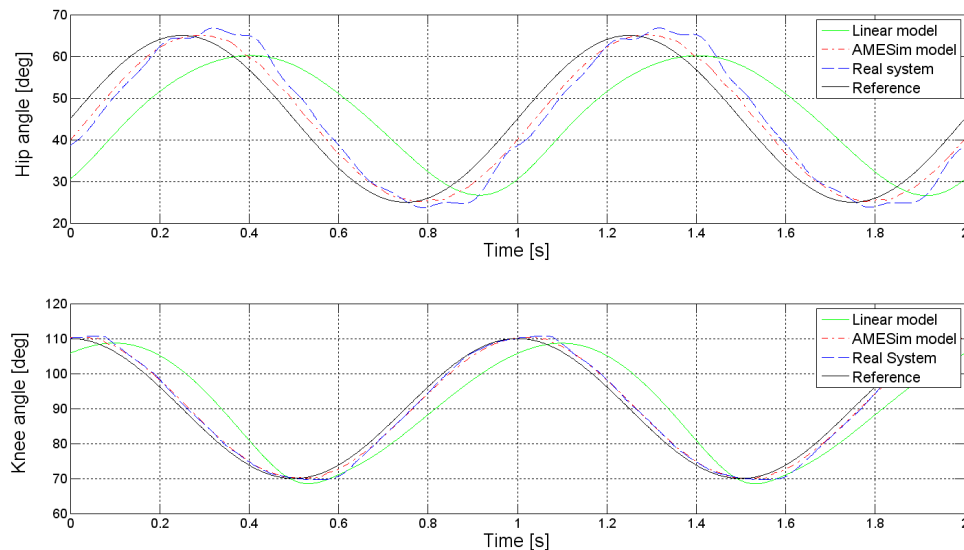


Figure 8. Sine tracking response for linear and non-linear (AMESim) models and the real system

A comparison between the tracking performance of the linear and non-linear models with respect to the real system was carried out and is depicted in Fig. 8. The non-linear model captures very well the response of the real system. On the contrary, the tracking error of the linear model is much bigger, due to the approximations and the above mentioned scaling factors.

In order to compare the performance of the proposed control architectures, the bio-inspired trajectory of Fig. 5 was used as reference. Different integral performance criteria were used to characterise the trajectory tracking responses, namely integrated error (IE), integrated absolute error (IAE), and integrated squared error (ISE) (Åström and Hägglund, 1995). The results are shown in Tab. 3 and in Fig. 9.

Table 3. Comparison of trajectory following performance of classic PID vs. PID with gain scheduling, using different integral performance criteria (for one period).

	PID		PID with gain scheduling	
	Hip	Knee	Hip	Knee
IE	0.91	-0.38	-0.29	-0.34
IAE	17.69	9.58	16.77	9.83
ISE	193.07	63.80	181.18	67.15

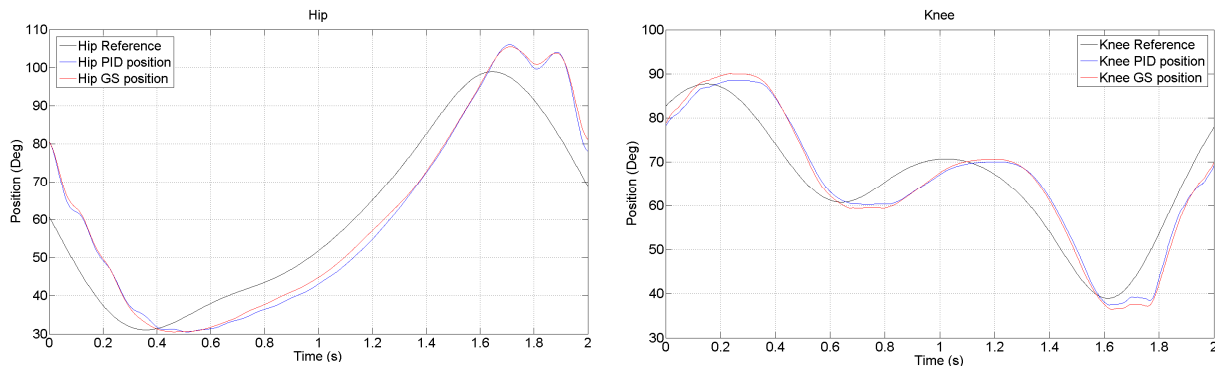


Figure 9. Comparison of trajectory following performance of classic PID vs. PID with gain scheduling (GS)

## 6. CONCLUSIONS AND PROPOSALS FOR FURTHER WORK

A linear and a non-linear model of a hydraulically actuated robot leg and its hydraulic actuation system have been developed and system performance predicted using simulation. An experimental validation of the simulation study has been undertaken on the valve and on the whole system. While the linear model is not very accurate, the non-linear model of the system describes the measured behaviour sufficiently well.

A PID controller has been initially tuned based on the linear model of the system. Its performance were not satisfactory because of the approximation of the linear model (*e.g.*, the joint variable load force in the hydraulic actuator, the mutual influence of each joint, and the Coulomb and stiction friction terms were neglected) as well as uncertainty of estimated parameters (*e.g.*, viscous friction and cylinder leakage coefficients). Hence the PID was re-tuned and has been shown that good tracking capabilities can be achieved.

In order to improve the controller performance, a gain scheduling controller has been designed based on the joint position within an animal walking trajectory cycle. Its performance, with respect to the conventional PID controller, was slightly superior to the hip joint and a little inferior to the knee joint. Due to its more complicated design and complexity to implement it in the software, this controller scheme is questionable for the HyQ leg in the current development stage. Nonetheless, an adaptive control proposal is promising in a further leg development stage, when the ground contact and the locomotion mode (walking, running, hopping) will be considered.

In further studies, the linear model can be improved in order to obtain a better performance with respect to the real leg dynamics. This can be achieved with a MIMO approach as opposed to the decoupled SISO approach used. Other linear control schemes such as pole placement and the linear-quadratic regulator (LQR) could be tested as well. Moreover, non-linear control techniques such as feedback linearisation and sliding control can be investigated. The subsequent steps in the project are the extension of the control to the whole robot with four legs, taking into account roll, pitch and yaw dynamics and studying its stability under various terrain conditions. Furthermore, the critical issue of the trade-off between power consumption, bandwidth and control performance will be addressed in further works by consideration of alternative flow modulation schemes.

## 7. REFERENCES

- Åström, K. J., & Hägglund, T., 1995, "PID controllers: theory, design and tuning", Instrument Society of America.
- Bentivegna, D. C., Atkeson C. G., & Kim, J-Y, 2007, "Compliant Control of a hydraulic humanoid joint", IEEE-RAS 7th Int. Conf. on Humanoid Robots (Humanoids 07), Pittsburgh, PA, USA.
- De Negri, V. J., Ramos Filho, J. R. B., Souza, A. D. C. De, 2008, "A Design Method for Hydraulic Positioning Systems" National Conf. on Fluid Power (NCFP), in conjunction with IFPE, Las Vegas, USA
- Hoyt, D. F., & Taylor, R. C., 1981, "Gait and the energetics of locomotion in horses", *Nature*, 292 (5820), 239-240.
- Hyon, S., Emura T., & Mita, T., 2003, "Dynamics-based control of one-legged hopping robot. *Journal of Systems and Control Engineering*", 217(2), April, pp. 83-98.
- Hayward, V., 1994, "Design of hydraulic robot shoulder based on combinatorial mechanism", *Experimental Robotics 3*, T. Yoshikawa and F. Miyazaki, Eds. Springer Verlag, pp. 297-310.
- Hyon S-H., & Cheng, G., 2006, "Gravity compensation and full-body balancing for humanoid robots", IEEE-RAS Int. Conf. on Humanoid Robotics, pp. 214-221.
- Hyon S-H., & Cheng, G., 2006, "Passivity-based full-body force control for humanoids and application to dynamic balancing and locomotion", IEEE/RSJ Int. Conf. on Intelligent Robots and Systems, pp. 4915-4922.
- Hyon S-H., & Cheng, G., 2007, "Simultaneous adaptation to rough terrain and unknown external forces for biped humanoids", IEEE-RAS 7th Int. Conf. on Humanoid Robots (Humanoids 07), Pittsburgh, PA, USA.
- Jacazio, G., & Bassolini, G., 2005, "A high performance force control system for dynamic loading of fast moving actuators", Proc. Bath Workshop on Power Transmission and Motion Control, Bath, UK.
- Jarrah, M. A. & Al-Jarrah, O. M., 1999, "Position control of a robot manipulation using continuous gain scheduling", IEEE Int. Conf. on Robotics and Automation, pp. 170-175.
- Kachroo, P., & Tomizuka, M., 1996, "Chattering reduction and error convergence in the sliding mode control of a class of nonlinear systems", *IEEE Trans. Automatic Control*, 41(7).
- Krus, P. & Gunnarson, S., 1993, "Adaptive control of a hydraulic crane using on-line identification", Proc. Third Scandinavian Conf. on Fluid Power, Linköping, Sweden.
- Levine, W. S., 1995, "The control handbook", CRC Press
- Linjama, M., & Virvalo, T., 2005, "Low-order robust controller for flexible hydraulic manipulators", Proc. Bath Workshop on Power Transmission and Motion Control, Bath, UK.
- Liston, R. A. & Mosher, R. S., 1968, "A Versatile Walking Truck", Transportation Engineering Conference.
- Luca, A. D., Albu-Schaffer, A., Haddadin, S. & Hirzinger, G., 2006, "Collision detection and safe reaction with the dlr-iii lightweight manipulator arm", IEEE/RSJ Int. Conf. on Intelligent Robots and Systems, pp. 1623-1630.
- Merritt, H., 1967, "Hydraulic Control Systems", John Wiley & Sons.
- Namvar, M., & Aghili, F., 2003, "A combined scheme for identification and robust torque control of hydraulic actuators", *Journal of Dynamic Systems, Measurement, and Control*, vol. 125, pp. 595-606, 2003.
- Paijmans, B., Symens, W., Brussel, H. V., & Swevers, J., 1999, "Gain scheduling control for mechanics systems with position dependent dynamics", Int. Conf. on Noise and Vibration Engineering, pp. 170-175.
- Palli, G., Melchiorri, C., Wimbock, T., Grebenstein, M. & Hirzinger, G., 2007, "Feedback linearization and simultaneous stiffness-position control of robots with antagonistic joints", IEEE/RSJ Int. Conf. on Robotics and Automation, Rome, Italy, April 2007, pp. 1623-1630.
- Raibert, M., Brown, H. J., & Chepponis, M., 1984, "Experiments in balance with a 3D one-legged hopping machine", *International Journal of Robotics Research*, 3(2), pp. 75-92.
- Raibert, M., Brown, H. J., 1984, "Experiments in balance with a 2D one-legged hopping machine", *Journal of Dynamic Systems, Measurement and Control*, 106, pp. 75-81.
- Raibert, M., Blankespoor K., Nelson, G., Playter, R. & the BigDog Team, 2008, "BigDog, The Rough-Terrain Quadruped Robot", Proceedings of 17<sup>th</sup> World Congress. The Int. Federation of Automatic Control, Seoul, Korea, pp. 10822-10825.
- Sakakibara, Y., Kan, K., Hosoda, Y., Hattori, M., & Fujie, M., 1990, "Foot trajectory for a quadruped walking machine", IEEE Int. Conf. on Intelligent Robots and Systems, pp. 315-322.
- Semini, C., Tsagarakis, N. G., Vanderborght, B., Yang Y., & Caldwell, D. G., 2008, "HyQ – hydraulically actuated quadruped robot: hopping leg prototype", IEEE/RAS Int. Conf. on Biomedical Robotics and Biomechanics (Biorob), pp. 593-599.

## 8. RESPONSIBILITY NOTICE

The authors are the only responsible for the printed material included in this paper.